Journal of Inflammation Research

Dovepress
Taylor & Francis Group

Open Access Full Text Article

ORIGINAL RESEARCH

Yin-Hua Li-Shi Formula Exerts Anti-Atopic Dermatitis Effects Through Luteolin Targeting AKT/MAPK-IL-6/IL-17 Axis

Xuemin Wang[1,*], Ning Jia[2,*], Hyewon Joo[3,*], Shuxin Wang[4], Caiyun Zhang[2], Qilong Chen[2], Wencheng Jiang[1]

[1]Department of Traditional Chinese Medicine Dermatology, Shanghai Skin Disease Hospital, School of Medicine, Tongji University, Shanghai, 200443, People's Republic of China; [2]Central Laboratory, Shanghai Skin Disease Hospital, School of Medicine, Tongji University, Shanghai, 200443, People's Republic of China; [3]Allergic Dermatoses Clinical Center, Shanghai Skin Disease Hospital, Tongji University School of Medicine, Shanghai, 200443, People's Republic of China; [4]Guang'anmen Hospital, China Academy of Chinese Medical Sciences, Beijing, 100053, People's Republic of China

*These authors contributed equally to this work

Correspondence: Wencheng Jiang; Qilong Chen, Shanghai Skin Disease Hospital, Tongji University School of Medicine, Shanghai, 200443, People's Republic of China, Email drjiangwencheng@163.com; cqlw1975@126.com

Background: Yin-Hua Li-Shi Formula (YHLS), a medically authorized traditional Chinese medicine (TCM) formulation for atopic dermatitis (AD), has a 30-year clinical application history in China, yet has not had its precise therapeutic mechanisms fully elucidated to date.

Methods: Chemical profiling of YHLS was conducted using high-performance liquid chromatography-tandem mass spectrometry (UPLC-MS/MS). Network pharmacology predicted YHLS's active ingredients, therapeutic targets, and anti-atopic dermatitis (AD) pathways, with molecular docking validating component-target binding affinity. By intersecting network pharmacology/molecular docking results with mass spectrometry profiles, the key bioactive component was identified. For in vivo validation, an AD-like model was generated via topical MC903 application in C57BL/6 mice. Dermatitis severity, ear thickness, H&E staining, ELISA, RT-qPCR, and Western blot were performed to assess YHLS's efficacy and underlying mechanisms.

Results: Luteolin, the major bioactive component of YHLS targeting AD, was identified by intersecting UPLC-MS/MS metabolite profiles with network pharmacology and molecular docking results. Network pharmacology revealed 102 common targets between YHLS and AD, with PPI/KEGG analyses confirming MAPK1 and AKT1 as core inflammatory targets. Molecular docking assays demonstrated that luteolin binds tightly to MAPK1 (−8.2 kcal/mol) and AKT1 (−9.7 kcal/mol). In MC903-induced AD-like mice, YHLS alleviated symptoms dose-dependently (reduced severity scores, ear thickness, hyperkeratosis, and inflammatory infiltration; all $P<0.05$). High-dose YHLS decreased serum IgE ($P<0.001$) and inhibited AKT1/MAPK1 phosphorylation. RT-qPCR showed YHLS downregulated IL-6 (high-dose $P<0.05$) and potently suppressed IL-17 (all doses $P<0.0001$, dose-dependent), with TNF-α also reduced.

Conclusion: Luteolin is the major bioactive component of Yin-Hua Li-Shi Formula (YHLS) that mediates its anti-atopic dermatitis effects by specifically targeting the AKT/MAPK-IL-6/IL-17 axis.

Keywords: atopic dermatitis, AD, Yin-Hua Li-Shi formula, YHLS, network pharmacology, molecular docking, animal experiment, inflammation, AKT/MAPK pathway

Introduction

Atopic dermatitis (AD) is a prevalent chronic inflammatory cutaneous disorder with a substantial global incidence,[1] which severely compromises patients' quality of life.[2] With respect to disability-adjusted life years (DALYs), atopic dermatitis represents the most burdensome skin disease globally, as reported by the Global Burden of Disease study. The condition affects approximately 15–20% of children and as many as 10% of adults.[3] This high prevalence, combined

https://doi.org/10.2147/JIR.S594212
Received: 11 February 2026
Accepted: 17 March 2026
Published: 25 March 2026

Graphical Abstract

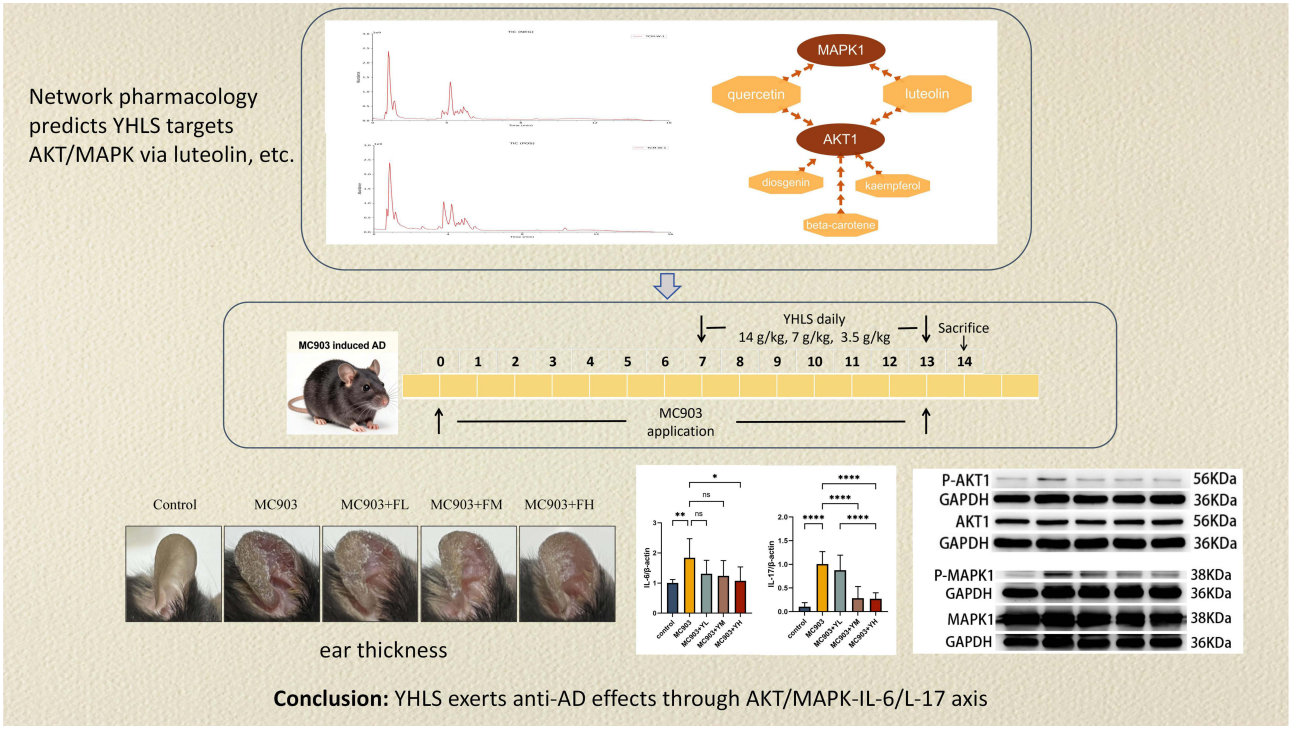

Conclusion: YHLS exerts anti-AD effects through AKT/MAPK-IL-6/L-17 axis

with its chronic, relapsing nature and significant quality-of-life impairment, underscores the urgent need for effective long-term treatment strategies for patients with AD.

The pathogenesis of AD involves multiple factors, including genetic predisposition, immune dysregulation, skin barrier dysfunction, and environmental exposures. Within this framework, dysregulated neuro-immune interactions are recognized as the central pathological hub. This core disturbance is further perpetuated by key auxiliary mechanisms, notably the itch-scratch cycle and disruptions to the cutaneous microbial ecosystem.[4,5] At the cellular level, the disease is primarily characterized by type 2 inflammation—predominantly driven by Th2 cells—alongside the aberrant activation of tissue-resident innate immune cells, including Langerhans cells and mast cells.[5] However, the inflammatory landscape is not limited to the Th2 axis; Increasing evidence suggests that Th1, Th17, and Th22 cells also exert crucial effects, especially in chronic AD, where they further disrupt immune homeostasis.[6,7] Such cellular dysregulation directly results in the aberrant secretion of various pro-inflammatory factors in AD.[4,8,9] Notably, two cytokines central to our experimental focus—IL-6 and IL-17—play pivotal roles in AD progression. IL-6, overexpressed by CD4+ T cells and keratinocytes in AD, and its receptor (IL-6R) has been linked to AD susceptibility via genetic studies.[10–13] As AD progresses from pre-lesional skin to acute and then chronic lesions, the inflammatory reactions linked to IL-17 undergo a progressive enhancement.[14,15]

The MAPK pathway is a pivotal mediator of pro-inflammatory signaling in AD. It transduces signals from dermal T cell-derived cytokines to stimulate keratinocytes to overproduce IL-33, which consequently disrupts the epidermal barrier and exacerbates the disease.[16] Meanwhile, AKT acts as a key intermediate in the IL-17/D-CD93 signaling axis, inhibiting DDX5 expression in keratinocytes via stepwise activation of the p38 MAPK-AKT-SMAD2/3 cascade; this disruption of DDX5 further alters IL-36R splicing balance, thereby amplifying IL-36R-mediated cutaneous inflammation and ultimately contributing to AD development.[17] These key pro-inflammatory factors and the AKT/MAPK pathways represent promising therapeutic targets for atopic dermatitis (AD) drug development, holding considerable clinical value.

Because of its persistent, recurring pattern, individuals with AD often need sustained, long-term treatment regimens. The traditional treatment for AD is systemic or local immunomodulators, including corticosteroids and calcineurin inhibitors, which although effective, are prone to drug resistance and have some adverse effects. In recent years, new drugs for the treatment of AD have been introduced one after another, such as biologics and JAK inhibitors.[18] They are effective and safe, offering a novel therapeutic option for patients with poor responses to traditional treatments—yet their high cost may impose a financial burden on patients, restricting widespread use.

The cost-effectiveness and immunomodulatory effects of natural medicines on skin diseases make them one of the potential therapeutic options worth exploring.[19] Yin-Hua Li-Shi Formula (YHLS) is a traditional Chinese medicine (TCM) formulation approved by medical institutions for atopic dermatitis (AD), with over 30 years of clinical application history in China. Wu et al have confirmed that it mitigates AD by modulating the Th1/Th2/Th17 cell balance and enhancing the expression of skin barrier-related proteins, including filaggrin (FLG) and loricrin (LOR).[20] It contains 6 Chinese herbs, JinYinHua (Lonicerae Japonicae Flos), Shanyao (Rhizoma Dioscoreae), Digupi (Lycii Cortex), Huangjing (Polygonati Rhizoma), Nvzhenzi (Fructus Ligustri Lucidi) and Yiyiren (Coicis Semen). YHLS has long been applied clinically for AD management, yet its specific chemical components and exact therapeutic mechanisms remain poorly understood.

Network pharmacology is a valuable tool for elucidating the therapeutic mechanisms of TCM formulations. In this study, we first combined this approach with UPLC-MS/MS analysis to identify the active components (with luteolin as the major bioactive ingredient) and candidate targets of YHLS, aiming to clarify its anti-AD mechanisms. We then established an MC903-induced AD-like model in C57BL/6 mice to evaluate the therapeutic efficacy of YHLS and validate the predicted core targets (MAPK, AKT) as well as the AKT/MAPK-IL-6/IL-17 signaling axis in vivo.

Materials and Methods

Preparation of YHLS

YHLS was formulated with 6 natural herbal medicines: 9g JinYinHua (*Lonicerae Japonicae Flos*), 9g Shanyao (*Rhizoma Dioscoreae*), 9g Digupi (*Lycii Cortex*), 9g Huangjing (*Polygonati Rhizoma*), 9g Nvzhenzi (*Fructus Ligustri Lucidi*), 9g Yiyiren (*Coicis Semen*). All herbal materials used in this study were purchased from Shanghai Caitongde Pharmaceutical Co., Ltd. (Shanghai, China) and were prepared according to the experimental requirements. The preparation process began by soaking the total 54 g of crude drugs in 270 mL of pure water (solid-to-liquid ratio 1:5) for 30 minutes. This was followed by a 30-minute decoction. After collecting the first decoction, the residue was re-extracted twice with an equal volume of pure water (ie., 3 consecutive extractions total). All aqueous extracts were combined and concentrated to a final volume of 38.5 mL, yielding a high-dose solution with a crude drug concentration of 1.4 g/mL. The medium- and low-dose solutions (0.7 g/mL and 0.35 g/mL, respectively) were obtained by diluting the high-dose preparation accordingly. All prepared YHLS samples were stored at 4°C until further use.

UPLC-MS/MS Analysis of YHLS for Quality Control

The chemical profile of YHLS was characterized using ultra-performance liquid chromatography-tandem mass spectrometry (UPLC-MS/MS) by Shanghai Luming Biological Technology Co., Ltd. Chromatographic separation was performed on an ACQUITY UPLC HSS T3 column, and mass spectrometric detection was conducted on a Thermo Orbitrap QE HF system. Detailed parameters are provided in Supplementary Table S1.

Predicting the Therapeutic Mechanism of YHLS for AD via Network Pharmacology Analysis

Target Screening

Active ingredients of the six YHLS herbs and their targets were retrieved from the TCMSP database, filtered by oral bioavailability (OB $\geq$ 30%) and drug-likeness (DL $\geq$ 0.18). AD-related targets were obtained from GeneCards. Targets of YHLS were then cross-referenced with established AD signature genes, and the overlapping targets were visualized in

a Venn diagram. The intersecting targets represent the core targets through which YHLS exerts its therapeutic effects against AD.

Drug-Compound-Target Network

Bioactive constituents and key targets were imported into Cytoscape 3.9.1 to build a compound-target interaction network.

Protein-Protein Interaction (PPI) Network

YHLS-AD overlapping targets were submitted to the STRING database (Homo sapiens, confidence score ≥ 0.9) for PPI network construction, with disconnected nodes excluded. Cytoscape 3.9.1 was used for visualization, and topological parameters (Betweenness Centrality (BC), Closeness Centrality (CC), Degree Centrality (DC), Eigenvector Centrality (EC), Local Average Connectivity (LAC), Network Centrality (NC), and Information Content (IC)) were calculated via CytoNCA for target prioritization. After two rounds of screening (retaining genes above the median of each parameter), 6 core targets (JUN, TP53, IL1B, MAPK1, AKT1, RELA) were identified, forming a core subnetwork with 6 nodes and 56 edges.

GO Enrichment Analysis and KEGG Enrichment Analysis

We performed Kyoto Encyclopedia of Genes and Genomes (KEGG) and Gene Ontology (GO) enrichment analysis through "ClusterProfiler" R package, with the screening criterion of $P < 0.05$, and the results were analyzed visually through SRplot (https://www.bioinformatics.com.cn/srplot).

KEGG-Target Network

To screen the core targets of YHLS in treating AD, the KEGG-Target network was established based on the top 16 most significantly enriched KEGG pathways and their associated target genes. The 5 targets with the highest degree values in this network were subsequently defined as its core targets.

Molecular Docking Validation

Core targets shared between the PPI network and the KEGG-Target network—specifically MAPK1 and AKT1—were selected as key therapeutic targets of YHLS against AD. MAPK1 and AKT1 were downloaded from PDB (https://www.rcsb.org/) in PDB format (resolution accuracy < 2.50A, 7≤PH≤8). The original ligand of the Discovery Studio 2019 Client complex was extracted and then re-connected to the active pocket of the complex. The Root Mean Square Deviation (RMSD) between the conformation of the ligands after docking and that in the original crystal structure was calculated. Select protein complexes with RMSD≤ 2.00A: MAPK1 (ID:6G97) and AKT1 (ID:4EJN).[21] According to the Compound-Target Network, the traditional Chinese medicine compound ingredients that act on the above two targets can be obtained, and their SDF format files were retrieved from the PubChem database (https://www.ncbi.nlm.nih.gov/pccompound). Molecular docking was finally performed using the online tool CB Dock2.[22]

Animals, Induction of AD and Drug Treatment

This study was conducted following approval from the Animal Ethics Committee of Shanghai Skin Disease Hospital (No. 2025–144) and the ARRIVE guidelines. Thirty male C57BL/6 mice of 8-week-old (weighing 21.73 ± 0.98 g) were randomized into five groups (n=6): Control, MC903 model, and three MC903+YHLS treatment groups (low-YL, medium-YM, high-YH dose). AD was induced via daily ear application of MC903 (0.05 g/L, 20 μL/ear) for 14 days. From day 8–14, treatment groups were gavaged with YHLS at 3.5, 7, or 14 g/kg/day, while controls received water. On day 14, samples (blood and ear skin) were collected under isoflurane anesthesia.

Assessment of Dermatitis Severity and Ear Thickness

Daily photographs of the ears were taken to evaluate dermatitis severity and measure ear thickness. Severity was assessed employing four clinical signs: rash/hemorrhagic spots, localized edema, epidermal damage, and desquamation/dryness. Each sign was scored on a 0–3 scale (0: none, 1: mild, 2: moderate, 3: severe). The individual scores were summed to

yield a total skin severity score (range 0–12). Concurrently, ear thickness was monitored at a consistent site using a vernier caliper to quantify lesion progression.

Hematoxylin and Eosin (H&E) Staining

Mouse ear tissues from each group were fixed in 4% paraformaldehyde at a tissue-to-fixative ratio of 1:8–1:10. Subsequently, the samples were processed through routine histological procedures including dehydration, paraffin embedding, sectioning, and H&E staining by a commercial service provider. The stained sections were sealed and examined under a microscope for imaging and archival purposes.

Enzyme Linked Immunosorbent Assay (ELISA)

After collection, blood was incubated at room temperature for 1 h and centrifuged (3000 rpm, 10 min). The separated serum was stored at −80°C for subsequent assays. Serum total IgE concentrations were determined with a commercial mouse ELISA kit (JM-02339M1, JINGMEI BIOTECHNOLOGY) in strict accordance with the provided protocol.

RT-qPCR

Total RNA was extracted from mouse ear tissues using Trizol reagent, and its concentration was determined spectrophotometrically. Reverse transcription was performed with TransScript® All-in-One SuperMix. Quantitative PCR was carried out using PerfectStart® Green qPCR SuperMix on an ABI QuantStudio 1 instrument. The mRNA expression levels of IL-6, IL-17 and Tnf-α were assayed, normalized to the housekeeping gene ACTB (β-actin), and calculated using the 2-ΔΔCT method.

Western Blot Analysis (WB)

Total proteins were extracted from ear skin specimens preserved at −80°C using RIPA lysis buffer (BF0003, Powerful Biology) fortified with PMSF (BL507A, Biosharp) and phosphatase inhibitors (MB12707, Meilunbio) to prevent degradation. Protein concentrations were quantified via BCA assay kit (BF0026, Powerful Biology) prior to SDS-PAGE separation and transfer onto PVDF membranes. Membranes were blocked with 5% skim milk in TBST for 30 minutes, then incubated overnight at 4°C with primary antibodies: AKT1 (1:2000, ET1609-47), p-AKT1 (1:1000, ET1612-73), p-MAPK1 (1:1000, ER1903-01), GAPDH (1:5000, ET1601-4; all HUABIO) and MAPK1 (1:5000, 51,068-1-AP, PTG). After three 5-minute TBST washes, secondary antibody incubation was performed at room temperature for 30 minutes. Post additional TBST rinsing, protein bands were visualized with ECL substrate and quantified using ImageJ.

Statistical Analysis

Prism 10 (GraphPad Software Inc., USA) was used for all analyses. All data was expressed as the mean ± standard deviation (SD). One-way analysis of variance (ANOVA) was employed to assess statistical differences between groups. Two-way ANOVA was used to compare the differences between groups at different time points. Values of $P < 0.05$ were considered statistically significant.

Results

Compound Identification of YHLS

The total ion chromatograms (TICs) of YHLS, acquired via UPLC-MS/MS, are presented in Figure 1A (positive ion mode) and Figure 1B (negative ion mode). A total of 668 compounds were identified from the 6 herbs in YHLS, including 109 Carbohydrates and Glycosides (19.68%), 87 Phenylpropanoids (15.7%), 56 Terpenes (10.11%), 54 Flavonoids (9.75%) and other compound categories (Figure 1C). The top 10 most abundant compounds among the 668 metabolites identified are Betaine, Cryptochlorogenic acid, Oxoglutaric acid, Secologanic acid, alpha-lactose, Kukoamine A, Malic acid, 2-hydroxyethyl(propan-2-yl) azanium, Gluconic Acid, and Verbenalin (Figure 1D).

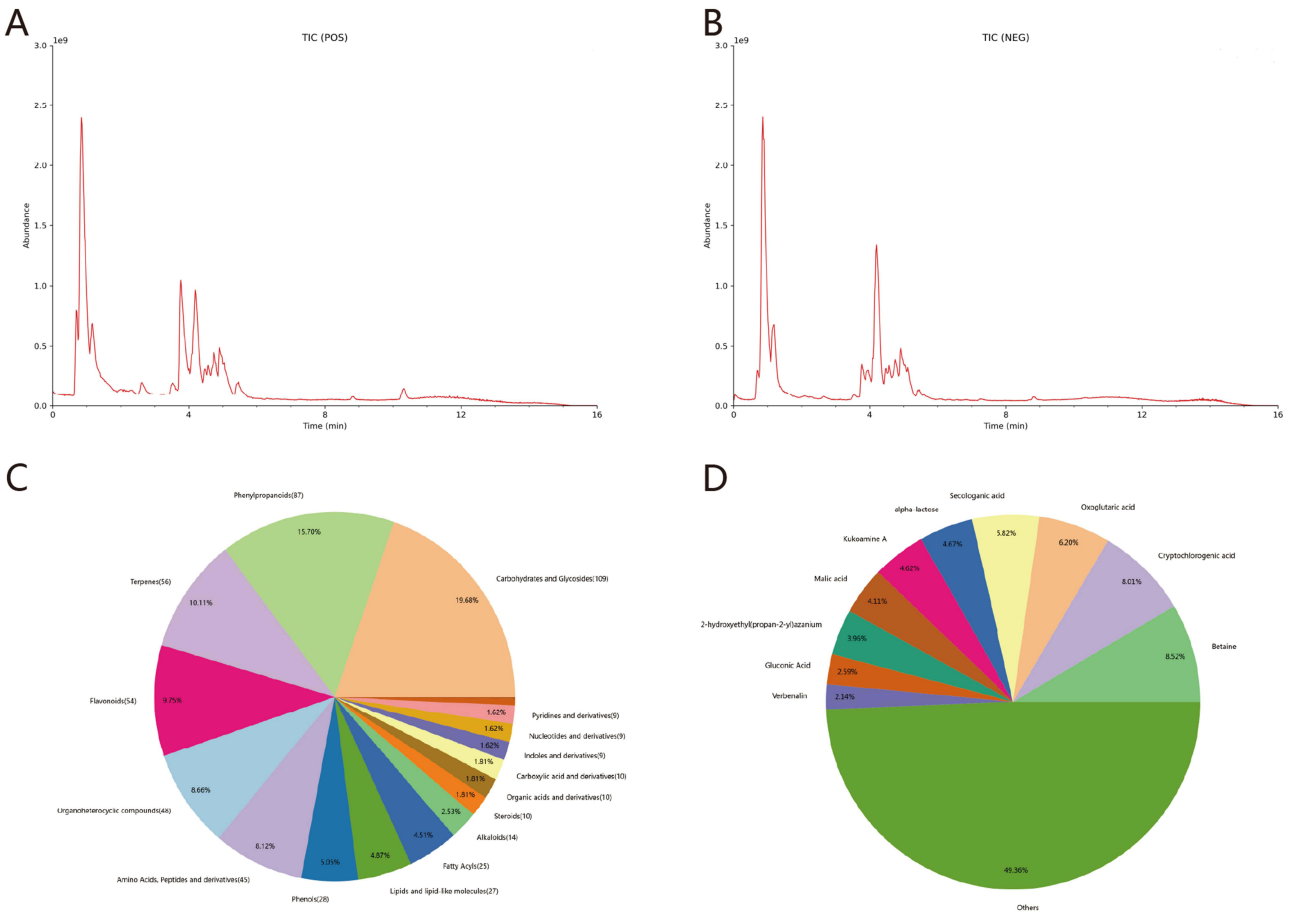

Figure 1 (**A** and **B**) TICs of YHLS. (**C**) The proportion distribution of each component in YHLS. (**D**) Distribution chart of the top 10 components in terms of content in YHLS.

Network Pharmacology Prediction Analysis

Target Screening and Drug-Ingredient-Target Network

Potential chemical components and AD-associated targets were identified following the procedures described earlier. Specifically, 1293 targets were linked to AD, while 295 targets were associated with YHLS; among these, 102 overlapping targets were designated as YHLS's potential therapeutic targets in AD treatment. (Figure 2A).

To visualize the interactions more clearly, a Drug-Component-Target Network was constructed (Figure 2B). In this network, different herbs in YHLS are distinguished by distinct colors: Yiyiren (Coicis Semen) is marked in orange, Nvzhenzi (Fructus Ligustri Lucidi) in red, Huangjing (Polygonati Rhizoma) in yellow, Shanyao (Rhizoma Dioscoreae) in blue, Digupi (Lycii Cortex) in green, and JinYinhua (Lonicerae Japonicae Flos) in purple.

GO and KEGG Pathway Enrichment Analysis

GO enrichment analysis (via DAVID) identified 1808 biological process, 33 cellular component, and 156 molecular function-related enriched terms. The top 10 terms in each category are shown in Figures 2C–E: the key biological processes (BP) term was "response to lipopolysaccharide", the core cellular components (CC) term was "membrane raft", and the primary molecular functions (MF) term was "RNA polymerase II-specific DNA-binding transcription factor binding".

To further clarify the therapeutic mechanism of YHLS against AD at the signaling pathway level, KEGG enrichment analysis was performed. This analysis revealed that the 88 candidate targets were significantly enriched in 174 pathways; the top 16 pathways (ranked by gene count, $P<0.05$) are presented in Figure 2F. Notably, several immune-related pathways (including TNF, IL-17, Th17, and PD-L1 signaling) were identified, implying that YHLS may alleviate AD by modulating immune responses.

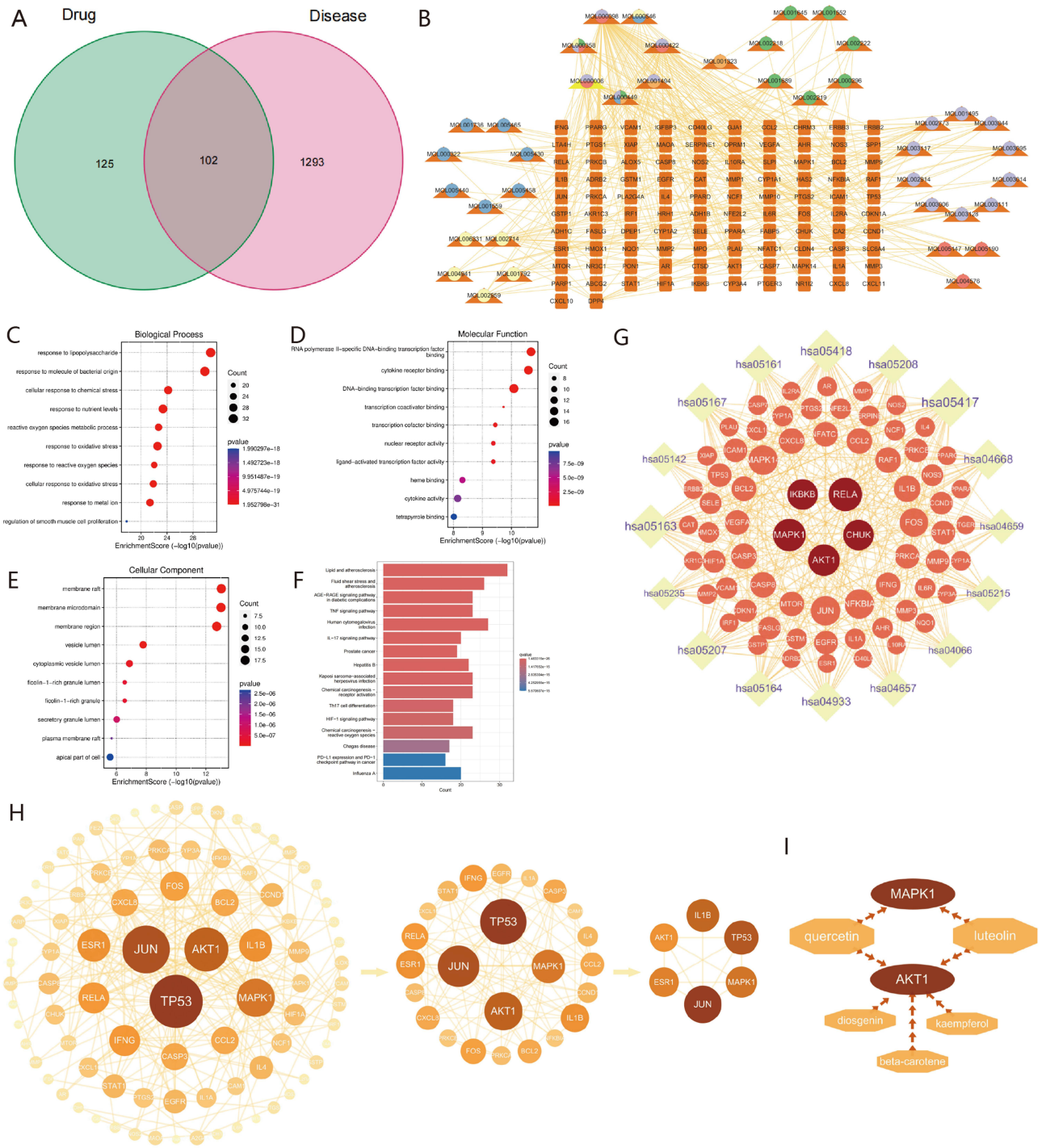

Figure 2 (**A**) Venn diagram depicting the overlap between active compound targets and AD-associated targets. (**B**) "Drug-Component-Target" interaction network, representing active YHLS constituents and their potential AD-related targets. (**C–E**) GO functional enrichment plots presenting the top 10 significantly enriched terms in the BP, CC, and MF categories, respectively. (**F**) Bar graph illustrating the 16 most significantly enriched KEGG pathways. (**G**) KEGG-Target pathway network, where crimson dots indicate the core targets in the K-T network. (**H**) PPI network of YHLS targets in AD treatment, along with the derivation of the core subnetwork via two rounds of scoring and filtering. In this network, gene importance is reflected by color intensity: darker shades correspond to higher functional significance. (**I**) Visualization of the key targets (MAPK1, AKT1) and the five YHLS-derived chemical components that interact with these targets.

KEGG-Target Network and K-T Core Targets

To identify key therapeutic targets, a KEGG-Target network was constructed based on the 102 overlapping targets of YHLS and AD (ie., the differentially expressed genes) and their associated KEGG pathways (Figure 2G), with KEGG

https://doi.org/10.2147/JIR.S594212

Table 1 Binding Energy Scores and Centre Coordinates of the Active Compounds Docked with the Key Target Proteins

Ligand	Protein	Affinity (kcal/mol)	Center (x, y, z)
Diosgenin	AKT1	−10.1	30, 43, 15
Beta-carotene	AKT1	−10.0	30, 43, 15
Kaempferol	AKT1	−9.4	30, 43, 15
Luteolin	AKT1	−9.7	30, 43, 15
Quercetin	AKT1	−9.7	30, 43, 15
Luteolin	MAPK1	−8.2	2,8,45
Quercetin	MAPK1	−8.3	2,8,45

pathways represented by yellow diamonds and target genes by orange/crimson dots. According to "degree", the top five target proteins (ie., KEGG-Target core targets) are RELA, MAPK1, AKT1,CHUK and IKBKB.

PPI Network and PPI Core Targets

Using the STRING database, a PPI network of the 88 candidate targets was generated as described above. The confidence score was set to 0.90 or higher, and isolated nodes were removed during network construction. In this network, nodes with darker colors and larger sizes correspond to proteins that may play more critical roles in AD treatment.For further target prioritization, topological parameters (BC, CC, DC, EC, LAC, NC, and IC) were calculated via CytoNCA to score and filter targets. Only genes exceeding the median value of each parameter were retained, and this scoring-filtering process was repeated twice. Ultimately, 6 core target genes (JUN, TP53, IL1B, MAPK1, AKT1, RELA) were identified, forming a subnetwork with 6 nodes and 56 edges (Figure 2H).Subsequently, the core targets from the K-T network and the PPI network were cross-referenced, yielding two key overlapping targets (MAPK1, AKT1). These results suggest that MAPK1 and AKT1 are likely the key targets through which YHLS mediates its therapeutic action against AD. (Figure 2I).

Through UPLC-MS/MS analysis, luteolin was identified as the major bioactive component in the YHLS formula. In addition, glycoside derivatives of quercetin (Quercetin 3-(6"-malonylglucoside) and Quercetin 3-sambubioside) and glycoside derivatives of kaempferol (Kaempferol 3-neohesperidoside, 6-Hydroxykaempferol 3,6-diglucoside, and Kaempferol 3-rutinoside-7-rhamnoside) were also detected. Free quercetin, kaempferol, diosgenin, and beta-carotene were not detected in the extract.

Molecular Docking

From the PPI and KEGG-Target networks, the two key target proteins (MAPK1, AKT1) and their matched active components were identified, and molecular docking verification was subsequently performed.

The docking results demonstrated strong binding affinity, with all compound-target pairs exhibiting binding energies below –8.0 kcal/mol (Table 1). The three-dimensional conformations of each component-target pair are visualized in Figures 3A–G. Furthermore, the docking plots of these pairs implied potential intermolecular interactions between the key components and target proteins.

Experimental Validation of Network Pharmacology Findings

YHLS Attenuates the Inflammatory Phenotype in MC903-Induced AD Model

Photographic records showed that topical MC903 application elicited characteristic AD-like cutaneous lesions, characterized by severe erythema, erosion, xerosis, edema, and scaling. Dermatitis scores were substantially elevated in the MC903 group compared with the untreated controls. After 3 days of intervention, the MC903+FH (high-dose YHLS) group exhibited alleviated symptoms (rash/hemorrhagic spots, localized edema, epidermal damage, desquamation/dryness; $P<0.05$). By day 5 of treatment, all YHLS-administered (low/medium/high dose) groups presented significantly lower dermatitis scores relative to the model group ($P<0.05$), indicating a dose-dependent reduction in dermatitis severity.

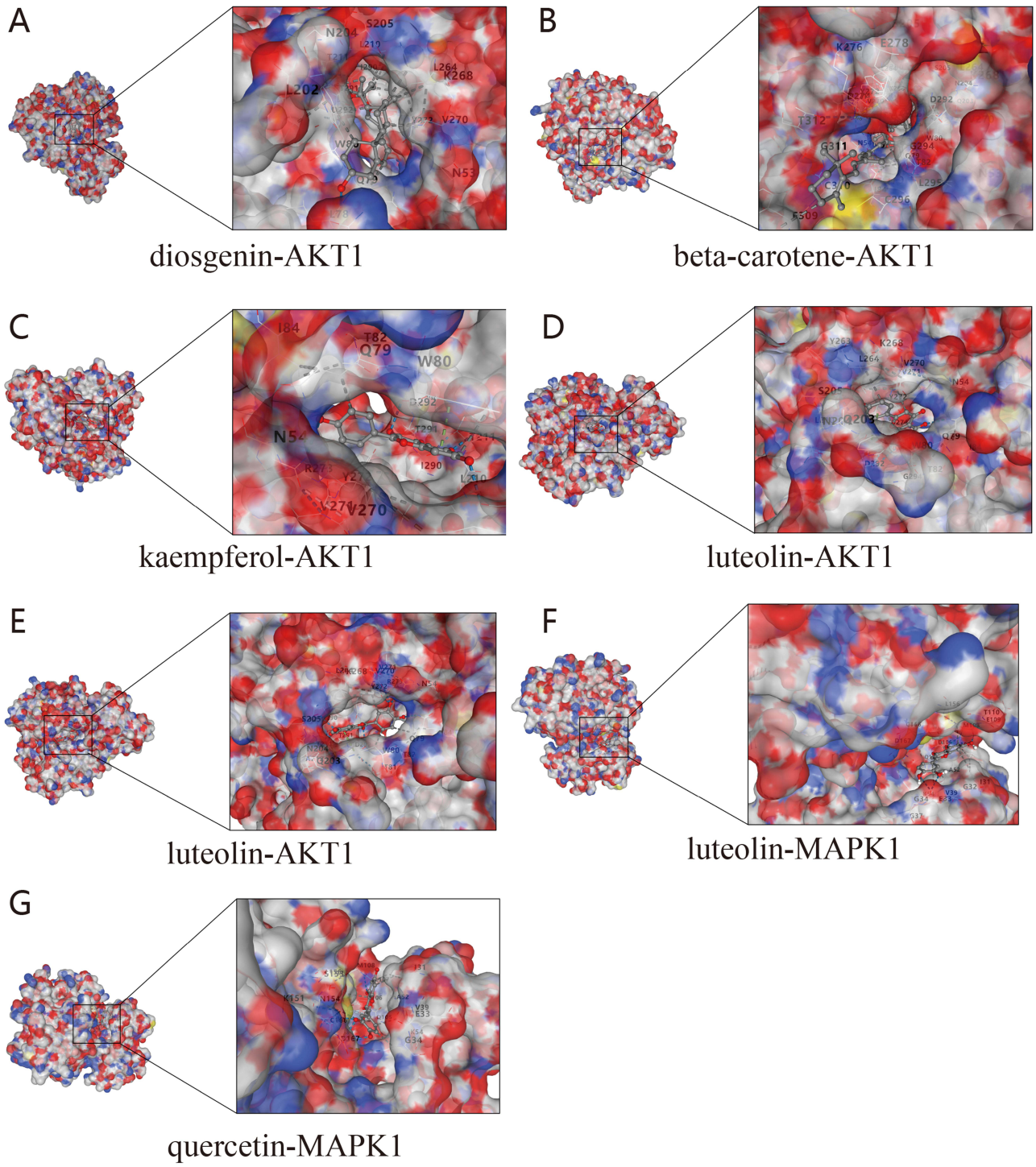

Figure 3 Schematic illustrations of molecular docking between core components of YHLS and key target proteins. Specifically, the docking complexes of diosgenin-AKT1, beta-carotene-AKT1, kaempferol-AKT1, luteolin-AKT1, quercetin-AKT1, luteolin-MAPK1, and quercetin-MAPK1 are corresponding to subpanels (**A–G**) in sequence.

Concurrently, ear thickness in YHLS-treated groups (high/medium/low dose) was markedly decreased relative to the model group ($P<0.05$), with the high-dose cohort demonstrating the most prominent improvement. These results further supported the dose-dependent anti-inflammatory effect of YHLS in relieving AD-related symptoms (Figure 4A, C, D).

H&E staining of ear sections revealed that MC903-induced AD mice exhibited characteristic pathological alterations, including hyperkeratosis, parakeratosis, acanthosis, and inflammatory cell infiltration, accompanied by a significant

https://doi.org/10.2147/JIR.S594212

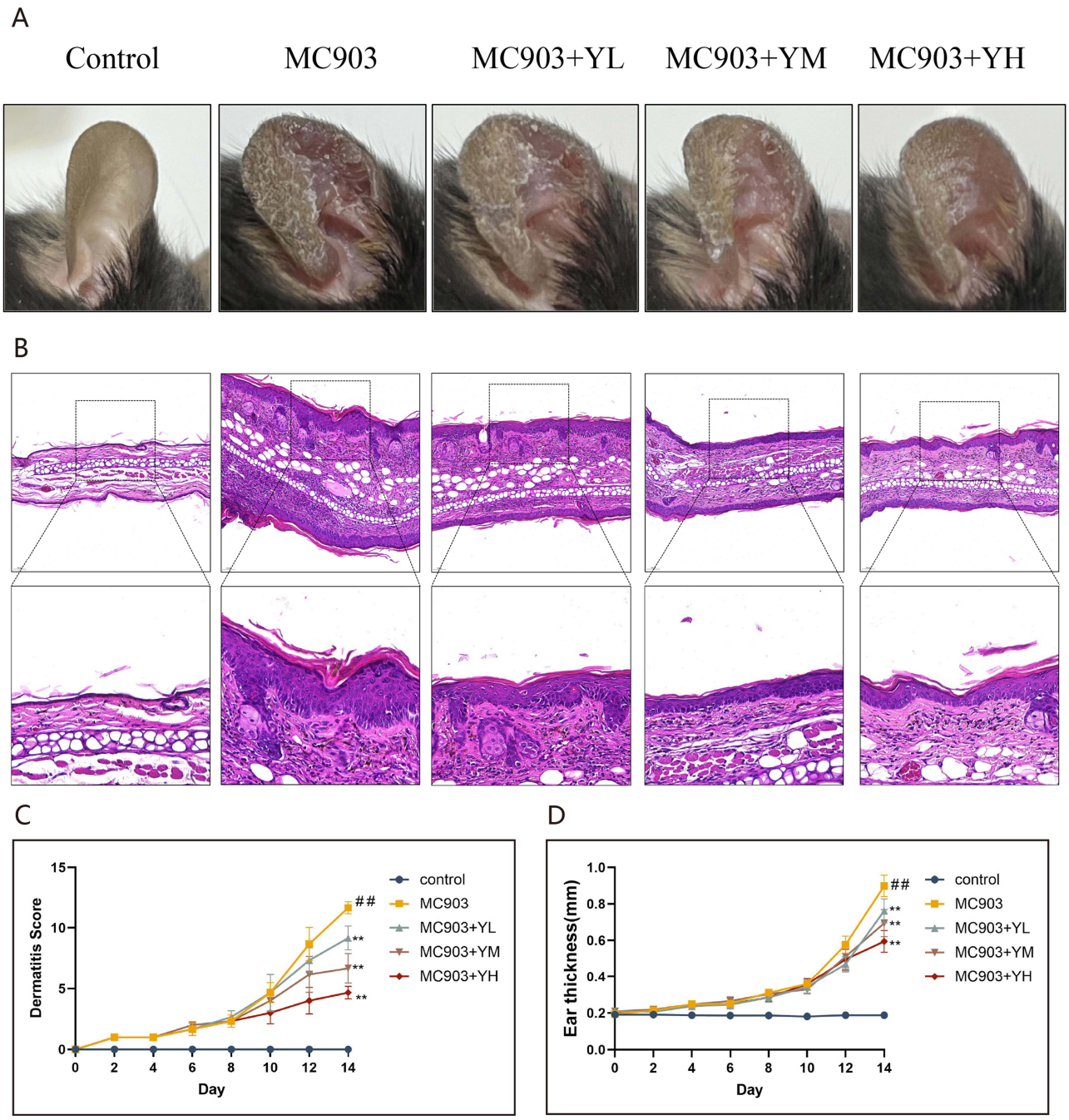

Figure 4 Therapeutic impact of YHLS on clinical and histopathological manifestations in MC903 induced AD mice. (**A**) Representative photographs of ear skin lesions. (**B**) Representative H&E stained. (**C**) Quantitative analysis of Dermatitis scores. (**D**) Quantitative analysis of ear thickness. Data are expressed as means ± SEM (n = 6). ***P* < 0.01 vs MC903 group; ###*P* < 0.01 vs Control group.

increase in ear thickness. These pathological changes were significantly alleviated following oral administration of YHLS.(Figure 4B).

YHLS Modulates Key Immune Factors Levels in MC903-Induced C57BL/6 Mice

Based on network pharmacology predictions, we found that YHLS treats AD primarily by regulating the MAPK and AKT pathways to modulate immunity.Since these pathways critically regulate the production and activity of key immune factors in AD, we next examined their influence on pivotal immune factors, including immunoglobulin E (IgE) and the inflammatory cytokines IL-6, IL-17, and TNF-α.

Serum IgE levels, measured by ELISA, were significantly lower in all YHLS-treated groups (low-, medium-, and high-dose YHLS co-administered with MC903) compared to the MC903-only model (treated with MC903 alone without YHLS intervention).The reduction was dose-dependent: low- dose YHLS produced a marked decrease ($P < 0.001$), while medium- and high- dose groups exhibited even greater suppression (both $P < 0.0001$). (Figure 5A).

In ear tissue, IL-6 expression was significantly lowered only in the high-dose (MC903+YH) YHLS group ($P < 0.05$). Although the medium-dose (MC903+YM) and low-dose (MC903+YL) YHLS groups exhibited a downward trend in IL-6 levels, these changes did not reach statistical significance (ns, no significance) (Figure 5B). Regarding IL-17, a different regulatory pattern was observed. In contrast, all YHLS intervention groups (low-, medium-, and high-dose) presented markedly reduced IL-17 expression (all $P < 0.0001$). Notably, this inhibitory effect on IL-17 showed a clear dose-dependent manner: as the dose of YHLS increased, the decline in IL-17 levels became more pronounced. (Figure 5C). Similarly, TNF was also significantly decreased in the treatment group, with no significant dose dependency and comparable effects across the three dose groups. (Figure 5D).

Collectively, these results demonstrate that YHLS effectively downregulates IgE, IL-6, IL-17, and TNF-α in an MC903-induced AD model, with responses varying in dose sensitivity across different immune markers.

YHLS Modulates AKT1 and MAPK1 Phosphorylation in AD Skin Tissue

In the aforementioned results, we were excited to find that YHLS can inhibit the expression of the key immune factors, including IgE, IL-6, IL-17 and TNF-α in AD mice, which confirms that YHLS indeed exerts an immunosuppressive effect.[23] Network pharmacology predictions suggested that AKT and MAPK may serve as the pharmacodynamic targets of YHLS in AD treatment. Subsequent Western blot analysis of ear skin tissues revealed that the phosphorylation ratios

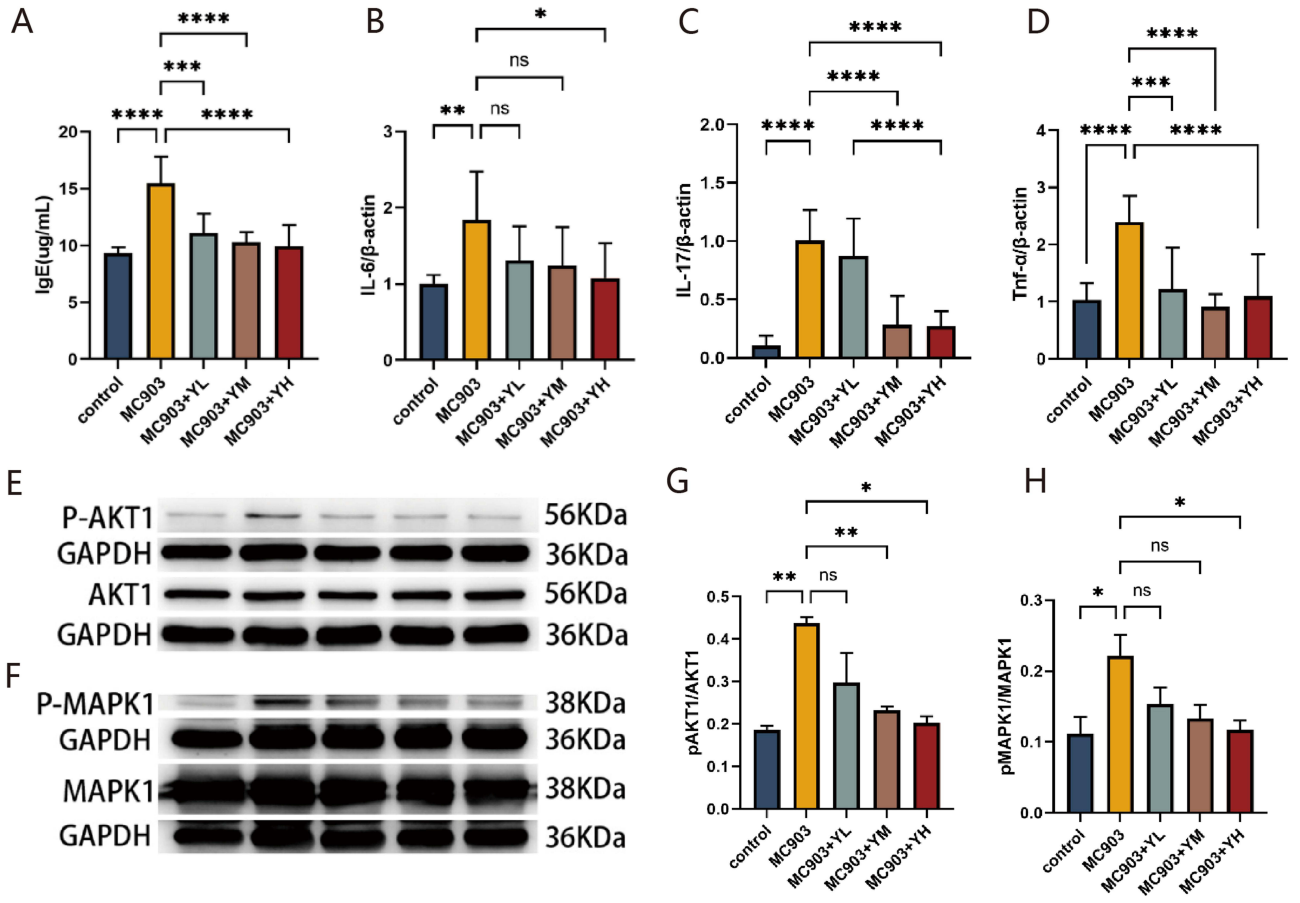

Figure 5 (**A**) Impact of YHLS on serum IgE levels: high-dose YHLS reduced serum IgE in MC903-induced mice (n=3). (**B–D**) YHLS-mediated changes in mRNA expression of IL-6, IL-17, and TNF-α in ear tissues. (**E** and **F**) Representative Western blot bands of p-AKT1, AKT1, p-MAPK1, MAPK1. (**G** and **H**) Quantitative analysis of p-AKT1/AKT1 and p-MAPK1/MAPK1 phosphorylation ratios. Data are expressed as mean ± SEM (n=3), *$P < 0.05$, **$P < 0.01$, ***$P < 0.001$ and ****$P < 0.0001$.

https://doi.org/10.2147/JIR.S594212

of AKT1 (p-AKT1/AKT1) and MAPK1 (p-MAPK1/MAPK1) were significantly elevated in the model group relative to controls. In contrast, these ratios were markedly reduced in a dose-dependent manner in YHLS-treated groups, in comparison with the model group. These results demonstrated that YHLS formula could treat MC903 induced AD-like symptoms by inhibiting p-AKT1 and p-MAPK1 expression (Figure 5E–H).

Discussion

AD is a prevalent, relapsing inflammatory skin condition defined by eczematous rashes and severe pruritus,[24] affecting up to 20% of the population and imposing a significant burden on quality of life.[25] Current treatments such as corticosteroids and biologics are limited by drug resistance, adverse effects, or high costs,[26] highlighting the need for effective and cost-efficient alternatives such as traditional Chinese medicine.[27–29]

YHLS is a clinically approved Chinese medicine formula with over 30 years of documented use in AD treatment, yet its precise pharmacodynamic mechanisms remain incompletely understood. In this study, a systematic research strategy was employed: UPLC-MS/MS was employed to characterize the chemical profile of YHLS; network pharmacology was applied to predict its potential therapeutic targets and pathways; molecular docking was used to validate the binding affinity of key components; and in vivo efficacy and mechanistic insights were verified in an MC903-induced AD mouse model. Integration of metabolomic data with network pharmacology predictions and molecular docking results identified luteolin as the primary bioactive component targeting AD. Taken together, our findings indicate that YHLS alleviates AD mainly through its key constituent luteolin, which modulates the AKT and MAPK signaling pathways, thereby suppressing the expression of downstream pro-inflammatory cytokines IL-6 and IL-17.

Network pharmacology-based KEGG enrichment analysis identified the TNF signaling pathway as a prominently enriched pathways mediating YHLS-induced anti-AD effects, which is consistent with the established role of TNF-α in propagating inflammatory cascades during AD development.[30,31] As a key pro-inflammatory cytokine,TNF-α activates diverse signaling cascades, such as NF-κB, MAPK, AKT, and JAK-STAT, which collectively drive the expression of inflammatory molecules, enhance immune cell infiltration, and impair skin barrier function.[32] Elevated TNF-α levels have been documented in both lesional skin and serum of AD patients relative to healthy individuals,[33,34] a finding further confirmed by our animal experiments: TNF-α and its downstream related pro-inflammatory cytokine IL-6 were significantly upregulated in our animal model. This observation suggests that YHLS may exert its therapeutic effects through TNF-α-related immune regulatory pathways. Notably, the PI3K-AKT and MAPK pathways are well-recognized downstream branches of the TNF signaling network: TNF-α can activate PI3K to induce AKT phosphorylation, or trigger the MAPK cascade through receptor binding, ultimately amplifying inflammatory responses and disrupting skin barrier integrity.[35,36] Our animal experiments verified that YHLS dose-dependently inhibited phosphorylation of AKT1 and MAPK1 in AD mouse skin tissues, providing direct evidence that YHLS may intervene in the TNF signaling network by inhibiting these two key downstream pathways, thereby blocking the transmission of inflammatory signals. In parallel, YHLS treatment lowered serum IgE, reduced mRNA levels of IL-6, IL-17 and TNF-α in ear tissues, mitigated clinical signs (eg., decreased dermatitis scores and ear thickness), and ameliorated histopathological features including hyperkeratosis. Together, these findings corroborate the proposed mechanism whereby YHLS alleviates AD through targeting the AKT/MAPK-IL-6/IL-17 axis.

MAPK1 (ERK2), a core member of the ERK subfamily, plays a pivotal role in AD pathogenesis by linking type 2 inflammation, epidermal barrier impairment, and pruritus—three hallmarks of AD. Moreover, p-ERK1/2 is strongly expressed in the skin of AD mice;[37] several studies have reported that drug intervention can improve AD symptoms by down-regulating the phosphorylation of ERK1/2 in MC903 mice.[38–40] Consistent with this established mechanism, our findings demonstrate that YHLS significantly downregulates p-MAPK1 expression in AD mice, confirming the clinical relevance of targeting ERK/MAPK1 for AD treatment. YHLS likely attenuates AD via several MAPK-dependent mechanisms: First, MAPK signaling promotes Th17 differentiation and IL-17 production;[41] the dose-dependent decline in IL-17 levels after YHLS administration, particularly at medium and high doses, implies that MAPK1 inhibition directly curbs Th17-driven inflammation; Second, previous studies have provided evidence that hyperactivated ERK signaling downregulates filaggrin and tight-junction proteins (eg., claudin-1) in keratinocytes,[37,42] which are are vital for ensuring the integrity of the skin barrier.[43] In line with this, our histological results showed alleviated hyperkeratosis and

epidermal thickening in YHLS-treated mice, indicating that YHLS may restore barrier function by inhibiting the MAPK pathway. Third, the ERK pathway contributes to pruritus regulation through endothelin-1, a key mediator of pruritus in AD,[44,45] potentially explaining the reduction of epidermal damage (likely resulting from scratching) observed in clinical symptom scoring.

As a member of the AKT kinase family, AKT1 participates in stabilizing epidermal barrier function. Its functional impairment is closely associated with parakeratosis in both AD patients and organotypic culture models.[46] Furthermore, AKT1 activation influences filaggrin expression, a key protein for skin barrier integrity.[47] In addition, clinically effective vitamin D therapy can repair the damaged skin barrier by inhibiting p-AKT1 expression to improve AD symptoms in mice.[48] Our results revealed that YHLS significantly decreased p-AKT1 levels in a dose-dependent manner, which may underlie its barrier-protective effects. Histological improvements, such as reduced hyperkeratosis, further support that YHLS restores filaggrin-mediated keratinocyte differentiation by inhibiting AKT1 and MAPK pathway. Concurrent with the modulation of AKT1 and MAPK1 phosphorylation, YHLS treatment markedly lowered IL-6 and IL-17 levels. IL-6, overexpressed by $CD4^+$ T cells in AD, contributes to multiple inflammatory processes and immune activation.[11,49] IL-17, predominantly secreted by Th17 cells, is a pivotal driver of inflammation in AD lesions.[50,51] Our findings demonstrate that YHLS effectively attenuates the activation of the MAPK and AKT signaling pathways. As key hubs of inflammatory signals, the inhibition of MAPK and AKT directly decreases the transcriptional production of the pro-inflammatory cytokine IL-6.[52] Moreover, IL-6 is a central cytokine that promotes the differentiation of naïve $CD4^+$ T cells into Th17 cells; thus, the reduction in IL-6, together with the direct inhibitory effect of MAPK/AKT blockade on T-cell differentiation, collectively diminishes IL-17 secretion.[53] Therefore, we have confirmed that YHLS effectively alleviates the inflammatory response of atopic dermatitis by targeting the MAPK/AKT-IL-6-IL-17 axis.

Based on the Drug-Ingredient-Target Network and animal experiments, we found that luteolin, quercetin act on AKT1 and MAPK1 while diosgenin, beta-carotene, kaempferol act on AKT1. These monomers have been reported to regulate the AKT or MAPK signaling pathways in inflammatory contexts.[54–59] Notably, luteolin, quercetin, beta-carotene, and kaempferol have been shown to improve AD by inhibiting inflammation and repairing the skin barrier.[60–63] Molecular docking further consistently demonstrated high-affinity interactions between these components and the target proteins, with all binding energies < –8.0 kcal/mol.

UPLC-MS/MS analysis verified that luteolin is the only component consistent with both network pharmacology predictions and actual detection, and it uniquely targets both AKT1 and MAPK1—this key consistency ensures our core mechanism conclusions remain unaffected. Free quercetin and kaempferol were not detected, which is consistent with our MS results showing their presence as glycosylated derivatives; while diosgenin and beta-carotene—both lipophilic compounds—were undetectable due to poor solubility in aqueous extracts. Although free quercetin and kaempferol were not detected in the YHLS extract, their glycosylated derivatives were identified by UPLC-MS/MS analysis. It is well-documented that these glycosylated derivatives can be biotransformed into their bioactive free aglycones (quercetin and kaempferol) in vivo, which may exert potential anti-AD effects through regulating the AKT/MAPK signaling pathway as well. Thus, the potential contribution of these glycosylated derivatives and their in vivo–generated free forms to the anti-AD efficacy of YHLS cannot be completely excluded. Notably, luteolin, as the major identified bioactive component in YHLS, directly targets both AKT1 and MAPK1 and fully covers the key signaling axis mediating the anti-AD effects, ensuring the core mechanistic conclusion of this study remains valid. Collectively, these findings suggest that YHLS improves atopic dermatitis symptoms by inhibiting the AKT and ERK pathways, an effect mediated by its bioactive components—luteolin, quercetin, diosgenin, beta-carotene, and kaempferol (Figure 6).

Conclusion

In conclusion, Yin-Hua Li-Shi Formula (YHLS) alleviates atopic dermatitis by modulating the AKT/MAPK-IL-6/IL-17 signaling axis, with luteolin identified as the key functional component.

Despite these findings, several research gaps remain. First, although luteolin was identified as a key bioactive compound through network pharmacology prediction, molecular docking, and chemical detection, the potential

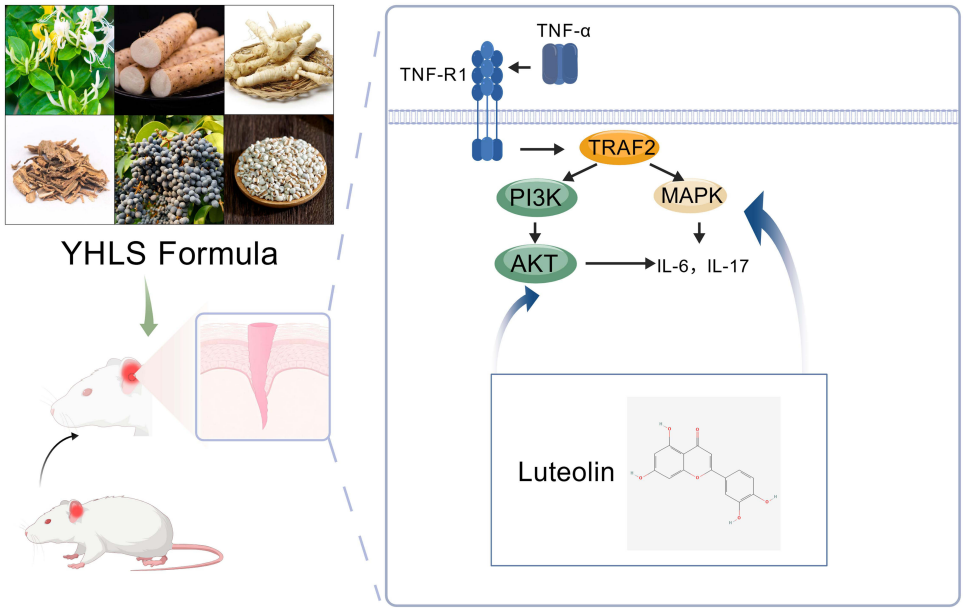

Figure 6 Schematic of the mechanism of YHLS compound targeting AKT and MAPK signaling pathways to reduce interleukin-6 and interleukin-17.[64]

synergistic interactions among multiple components of YHLS require further investigation. Second, the present study mainly relied on an MC903-induced AD mouse model, which may not fully recapitulate the complex immunopathological features of human atopic dermatitis. Future studies should therefore incorporate additional experimental models and human-derived cellular systems to further validate the underlying mechanisms. In addition, more in-depth studies are needed to elucidate the pharmacokinetic characteristics of the active constituents and to clarify how multi-component interactions collectively modulate the AKT/MAPK-IL-6/IL-17 axis. Such investigations will provide deeper insights into the pharmacological basis of YHLS and support its potential clinical application in the management of AD.

Data Sharing Statement

The data supporting the findings of this study are available upon reasonable request from the corresponding author.

Ethical Statement

All experimental procedures were approved by the Animal Ethics Committee of Shanghai Skin Disease Hospital (No.2025-144) and performed in compliance with ARRIVE guidelines.

Author Contributions

Xuemin Wang, Ning Jia, and Hyewon Joo contributed equally to this work and share first authorship.

Xuemin Wang[1], #:Conceptualization (contributed to the formulation of research goals), Methodology (participated in the design of experimental methods), Investigation (performed part of the animal experiments), Writing – original draft (drafted sections of the manuscript).

Ning Jia[2], #:Conceptualization (developed the overarching research aims), Formal analysis (conducted network pharmacology data analysis), Investigation (carried out molecular docking experiments), Writing – original draft (wrote the core mechanism sections).

Hyewon Joo[3], #:Data curation (managed and annotated research data), Visualization (prepared figures and tables), Investigation (assisted in animal experiment sample collection), Writing – review and editing (revised the manuscript for clarity).

Shuxin Wang[4]: Conceptualization (contributed to the development of the research concept and study design), Supervision (oversaw the overall research design and execution), Project administration (coordinated the research process), Writing – review and editing (critically revised the manuscript).

Caiyun Zhang[2]:Resources (provided laboratory reagents and animal models), Validation (verified the reproducibility of experimental results), Investigation (assisted in molecular experiment operations).

Qilong Chen[2] *:Methodology (optimized the network pharmacology analysis process), Writing – review and editing (revised the methodology section).

Wencheng Jiang[1]: Supervision (mentored the experimental implementation), Conceptualization (guided the research framework), Writing – review and editing (revised the manuscript for scientific rigor), Project administration (managed the research execution process).

All authors took part in drafting, revising or critically reviewing the article; gave final approval of the version to be published; have agreed on the journal to which the article has been submitted; and agree to be accountable for all aspects of the work.

Funding

This work was supported by the In-Hospital Research Project of Shanghai Dermatology Hospital (Grant No.: lcfy2024-09).

Disclosure

The authors declare no relevant financial or non-financial competing interests to report.

References

1. Guttman-Yassky E, Renert-Yuval Y, Brunner PM. Atopic dermatitis. *Lancet Lond Engl*. 2025;405(10478):583–596. doi:10.1016/S0140-6736(24)02519-4
2. Huang J, Choo YJ, Smith HE, Apfelbacher C. Quality of life in atopic dermatitis in Asian countries: a systematic review. *Arch Dermatol Res*. 2022;314(5):445–462. doi:10.1007/s00403-021-02246-7
3. Laughter MR, Maymone MBC, Mashayekhi S, et al. The global burden of atopic dermatitis: lessons from the global burden of disease study 1990–2017. *Br J Dermatol*. 2021;184(2):304–309. doi:10.1111/bjd.19580
4. Schuler CF, Tsoi LC, Billi AC, Harms PW, Weidinger S, Gudjonsson JE. Genetic and immunological pathogenesis of atopic dermatitis. *J Invest Dermatol*. 2024;144(5):954–968. doi:10.1016/j.jid.2023.10.019
5. Criado PR, Miot HA, Bueno-Filho R, Ianhez M, Criado RFJ, de Castro CCS. Update on the pathogenesis of atopic dermatitis. *An Bras Dermatol*. 2024;99(6):895–915. doi:10.1016/j.abd.2024.06.001
6. Savva M, Papadopoulos NG, Gregoriou S, et al. Recent advancements in the atopic dermatitis mechanism. *Front Biosci Landmark Ed*. 2024;29(2):84. doi:10.31083/j.fbl2902084
7. Eyerich K, Novak N. Immunology of atopic eczema: overcoming the Th1/Th2 paradigm. *Allergy*. 2013;68(8):974–982. doi:10.1111/all.12184
8. Li H, Zhang Z, Zhang H, Guo Y, Yao Z. Update on the pathogenesis and therapy of atopic dermatitis. *Clin Rev Allergy Immunol*. 2021;61(3):324–338. doi:10.1007/s12016-021-08880-3
9. Song A, Lee SE, Kim JH. Immunopathology and Immunotherapy of Inflammatory Skin Diseases. *Immune Netw*. 2022;22(1):e7. doi:10.4110/in.2022.22.e7
10. Corrêa MP, Areias LL, Correia-Silva RD, et al. The role of galectin-9 as mediator of atopic dermatitis: effect on keratinocytes. *Cells*. 2021;10(4):947. doi:10.3390/cells10040947
11. Toshitani A, Ansel JC, Chan SC, Li S-H, Hanifin JM. Increased interleukin 6 production by T cells derived from patients with atopic dermatitis. *J Invest Dermatol*. 1993;100(3):299–304. doi:10.1111/1523-1747.ep12469875
12. Esparza-Gordillo J, Schaarschmidt H, Liang L, et al. A functional IL-6 receptor (IL6R) variant is a risk factor for persistent atopic dermatitis. *J Allergy Clin Immunol*. 2013;132(2):371–377. doi:10.1016/j.jaci.2013.01.057
13. Zhao SS, Yiu ZZN. Genetically proxied IL-6 receptor inhibition is associated with increased risk of atopic dermatitis. *J Allergy Clin Immunol*. 2024;154(3):666–669. doi:10.1016/j.jaci.2024.05.016
14. Tsoi LC, Rodriguez E, Stölzl D, et al. Progression of acute-to-chronic atopic dermatitis is associated with quantitative rather than qualitative changes in cytokine responses. *J Allergy Clin Immunol*. 2020;145(5):1406–1415. doi:10.1016/j.jaci.2019.11.047
15. David E, Czarnowicki T. The pathogenetic role of Th17 immune response in atopic dermatitis. *Curr Opin Allergy Clin Immunol*. 2023;23(5):446–453. doi:10.1097/ACI.0000000000000926
16. Tsuji G, Yamamura K, Kawamura K, Kido-Nakahara M, Ito T, Nakahara T. Regulatory mechanism of the IL-33–IL-37 axis via aryl hydrocarbon receptor in atopic dermatitis and psoriasis. *Int J Mol Sci*. 2023;24(19):14633. doi:10.3390/ijms241914633
17. Ni X, Xu Y, Wang W, et al. IL-17D-induced inhibition of DDX5 expression in keratinocytes amplifies IL-36R-mediated skin inflammation. *Nat Immunol*. 2022;23(11):1577–1587. doi:10.1038/s41590-022-01339-3
18. Armario-Hita JC, Galán-Gutiérrez M, Dodero-Anillo JM, Carrascosa JM, Ruiz-Villaverde R. Updated review on treatment of atopic dermatitis. *J Investig Allergol Clin Immunol*. 2023;33(3):158–167. doi:10.18176/jiaci.0906

19. Goh BH, Mocan A, Xiao J, Mah SH, Yap WH. Editorial: targeting human inflammatory skin diseases with natural products: exploring potential mechanisms and regulatory pathways. *Front Pharmacol*. 2021;12:791151. doi:10.3389/fphar.2021.791151
20. Wu J, Tai Z, Zhu C, et al. Yin-Hua Li-Shi decoction alleviated atopic dermatitis through regulating th cells balance and restoring epithelial barrier. *J Inflamm Res*. 2025;18:14569–14587. doi:10.2147/JIR.S531656
21. Bagheri S, Behnejad H, Firouzi R, Karimi-Jafari MH. Using the semiempirical quantum mechanics in improving the molecular docking: a case study with CDK2. *Mol Inform*. 2020;39(9):e2000036. doi:10.1002/minf.202000036
22. Liu Y, Yang X, Gan J, Chen S, Xiao Z-X, Cao Y. CB-Dock2: improved protein–ligand blind docking by integrating cavity detection, docking and homologous template fitting. *Nucleic Acids Res*. 2022;50(W1):W159–W164. doi:10.1093/nar/gkac394
23. Facheris P, Jeffery J, Del Duca E, Guttman-Yassky E. The translational revolution in atopic dermatitis: the paradigm shift from pathogenesis to treatment. *Cell Mol Immunol*. 2023;20(5):448–474. doi:10.1038/s41423-023-00992-4
24. Langan SM, Irvine AD, Weidinger S. Atopic dermatitis. *Lancet*. 2020;396(10247):345–360. doi:10.1016/S0140-6736(20)31286-1
25. Weidinger S, Beck LA, Bieber T, Kabashima K, Irvine AD. Atopic dermatitis. *Nat Rev Dis Primer*. 2018;4(1):1–20. doi:10.1038/s41572-018-0001-z
26. Honda T. A new era in atopic dermatitis treatment and evolving therapeutic strategies. *Immunol Med*. 2025;1–13. doi:10.1080/25785826.2025.2567133
27. Zhang L, Lin H, Chen N, Zhu S, Hu Y. Selected traditional Chinese herbal medicines for the treatment of atopic dermatitis - research progress on the effect and mechanism of actions. *Front Pharmacol*. 2025;16:1553251. doi:10.3389/fphar.2025.1553251
28. Limantara NV, Sadono R, Widhiati S, Danarti R. Asian herbal medicine for atopic dermatitis: a systematic review. *Dermatol Rep*. 2023;16(1):9727. doi:10.4081/dr.2023.9727
29. Hussain Z, Thu HE, Shuid AN, Kesharwani P, Khan S, Hussain F. Phytotherapeutic potential of natural herbal medicines for the treatment of mild-to-severe atopic dermatitis: a review of human clinical studies. *Biomed Pharmacother Biomedecine Pharmacother*. 2017;93:596–608. doi:10.1016/j.biopha.2017.06.087
30. Banno T, Gazel A, Blumenberg M. Effects of tumor necrosis factor-α (TNFα) in Epidermal keratinocytes revealed using global transcriptional profiling*. *J Biol Chem*. 2004;279(31):32633–32642. doi:10.1074/jbc.M400642200
31. Howell MD, Kim BE, Gao P, et al. Cytokine modulation of atopic dermatitis filaggrin skin expression. *J Allergy Clin Immunol*. 2009;124(Suppl 3):R7–R12. doi:10.1016/j.jaci.2009.07.012
32. Purpurin suppresses atopic dermatitis via TNF-α/IFN-γ-induced inflammation in HaCaT cells - PubMed. Available from: https://pubmed.ncbi.nlm.nih.gov/35794850/. Accessed November 11, 2025.
33. Liu X, Luo Y, Chen X, et al. Fecal microbiota transplantation against moderate-to-severe atopic dermatitis: a randomized, double-blind controlled explorer trial. *Allergy*. 2025;80(5):1377–1388. doi:10.1111/all.16372
34. Clausen M-L, Kezic S, Olesen CM, Agner T. Cytokine concentration across the stratum corneum in atopic dermatitis and healthy controls. *Sci Rep*. 2020;10(1):21895. doi:10.1038/s41598-020-78943-6
35. Kalliolias GD, Ivashkiv LB. TNF biology, pathogenic mechanisms and emerging therapeutic strategies. *Nat Rev Rheumatol*. 2016;12(1):49–62. doi:10.1038/nrrheum.2015.169
36. Gao Z, Dai H, Zhang Q, Yang F, Bu C, Chen S. Hydroxytyrosol alleviates acute liver injury by inhibiting the TNF-α/PI3K/AKT signaling pathway via targeting TNF-α signaling. *Int J Mol Sci*. 2024;25(23):12844. doi:10.3390/ijms252312844
37. Z N, KN M, T G, et al. Role of ERK pathway in the pathogenesis of atopic dermatitis and its potential as a therapeutic target. *Int J Mol Sci*. 2022;23(7). doi:10.3390/ijms23073467
38. T J, L Y, C X, et al. CKBA suppresses mast cell activation via ERK signaling pathway in murine atopic dermatitis. *Eur J Immunol*. 2023;53(9). doi:10.1002/eji.202350374
39. Seshimo H, Egusa C, Maeda T, et al. Topical application of imatinib mesylate suppresses vitamin D3 analog-induced dermatitis in Balb/c mice. *Exp Dermatol*. 2023;32(4):413–424. doi:10.1111/exd.14720
40. Gu Y, Wang X, Liu F, et al. Total flavonoids of sea buckthorn (Hippophae rhamnoides L.) improve MC903-induced atopic dermatitis-like lesions. *J Ethnopharmacol*. 2022;292:115195. doi:10.1016/j.jep.2022.115195
41. Zhang J, Shen M. The role of IL-17 in systemic autoinflammatory diseases: mechanisms and therapeutic perspectives. *Clin Rev Allergy Immunol*. 2025;68(1):27. doi:10.1007/s12016-025-09042-5
42. IL-33 down-regulates CLDN1 expression through the ERK/STAT3 pathway in keratinocytes - PubMed. Available from: https://pubmed.ncbi.nlm.nih.gov/29534857/. Accessed October 6, 2024.
43. De Benedetto A, Rafaels NM, McGirt LY, et al. Tight junction defects in patients with atopic dermatitis. *J Allergy Clin Immunol*. 2011;127(3):773–777. doi:10.1016/j.jaci.2010.10.018
44. Kido-Nakahara M, Wang B, Ohno F, et al. Inhibition of mite-induced dermatitis, pruritus, and nerve sprouting in mice by the endothelin receptor antagonist bosentan. *Allergy*. 2021;76(1):291–301. doi:10.1111/all.14451
45. Aktar MK, Kido-Nakahara M, Furue M, Nakahara T. Mutual upregulation of endothelin-1 and IL-25 in atopic dermatitis. *Allergy*. 2015;70(7). doi:10.1111/all.12633
46. As N, Z Y, Wl D, M S, Rf O. AKT1-mediated Lamin A/C degradation is required for nuclear degradation and normal epidermal terminal differentiation. *Cell Death Differ*. 2015;22(12). doi:10.1038/cdd.2015.62
47. O'Shaughnessy RFL, Welti JC, Cooke JC, et al. AKT-dependent HspB1 (Hsp27) activity in epidermal differentiation. *J Biol Chem*. 2007;282(23):17297–17305. doi:10.1074/jbc.M610386200
48. L R, P Z, L P, et al. Vitamin D attenuates DNCB-induced atopic dermatitis-like skin lesions by inhibiting immune response and restoring skin barrier function. *Int Immunopharmacol*. 2023:122. doi:10.1016/j.intimp.2023.110558
49. Huang S, Wang H, Zheng H, et al. Association between IL-6 polymorphisms and atopic dermatitis in Chinese Han children. *Front Pediatr*. 2023;11:1156659. doi:10.3389/fped.2023.1156659
50. Liu T, Li S, Ying S, et al. The IL-23/IL-17 pathway in inflammatory skin diseases: from bench to bedside. *Front Immunol*. 2020;11:594735. doi:10.3389/fimmu.2020.594735
51. Hofmann MA, Fluhr JW, Ruwwe-Glösenkamp C, Stevanovic K, Bergmann K-C, Zuberbier T. Role of IL-17 in atopy—A systematic review. *Clin Transl Allergy*. 2021;11(6):e12047. doi:10.1002/clt2.12047

52. Jiang R, Tang J, Zhang X, et al. CCN1 promotes inflammation by inducing IL-6 production via α6β1/PI3K/AKT/NF-κB pathway in autoimmune hepatitis. *Front Immunol*. 2022;13:810671. doi:10.3389/fimmu.2022.810671
53. Hailemichael Y, Johnson DH, Abdel-Wahab N, et al. Interleukin-6 blockade abrogates immunotherapy toxicity and promotes tumor immunity. *Cancer Cell*. 2022;40(5):509–523.e6. doi:10.1016/j.ccell.2022.04.004
54. Hou B, Su S, Ji L, et al. Luteolin alleviates right ventricular hypertrophy in high altitude pulmonary hypertension rats by regulating PI3K/AKT/mTOR signalling pathway. *Eur J Pharmacol*. 2025;1003:177898. doi:10.1016/j.ejphar.2025.177898
55. Semmarath W, Arjsri P, Srisawad K, Umsumarng S, Dejkriengkraikul P. Luteolin-rich extract from *Harrisonia perforata* (Blanco) Merr. root alleviates SARS-CoV-2 spike protein-stimulated lung inflammation via inhibition of MAPK/NLRP3 inflammasome signaling pathways. *Life Basel Switz*. 2025;15(7):1077. doi:10.3390/life15071077
56. He H, Sun S, Zhang M, Shou L. Research on erchen tang in the treatment of community-acquired pneumonia based on chemical molecular mechanisms of quercetin and kaempferol: PI3K/AKT/NF-κB protein signaling. *Int J Biol Macromol*. 2025;311(Pt 4):144071. doi:10.1016/j.ijbiomac.2025.144071
57. Abu-Risha SE, Sokar SS, Elzorkany KE, Elsisi AE. Donepezil and quercetin alleviate valproate-induced testicular oxidative stress, inflammation and apoptosis: imperative roles of AMPK/SIRT1/PGC-1α and p38-MAPK/NF-κB/IL-1β signaling cascades. *Int Immunopharmacol*. 2024;134:112240. doi:10.1016/j.intimp.2024.112240
58. Hao-Peng YA, Lei YU, Qian LI, et al. Diosgenin inhibits tumor necrosis factor-induced tissue factor activity and expression in THP-1 cells via down-regulation of the NF-κB, Akt, and MAPK signaling pathways. *Chin J Nat Med*. 2013;11(6):608–615. doi:10.1016/S1875-5364(13)60070-9
59. Xu G, Ma T, Zhou C, Zhao F, Peng K, Li B. β-carotene attenuates apoptosis and autophagy via PI3K/AKT/mTOR signaling pathway in necrotizing enterocolitis model cells IEC-6. *Evid-Based Compl Altern Med ECAM*. 2022;2022:2502263. doi:10.1155/2022/2502263
60. Tang L, Gao J, Li X, Cao X, Zhou B. Molecular mechanisms of luteolin against atopic dermatitis based on network pharmacology and in vivo experimental validation. *Drug Des Devel Ther*. 2022;16:4205–4221. doi:10.2147/DDDT.S387893
61. Hou -D-D, Zhang W, Gao Y-L, et al. Anti-inflammatory effects of quercetin in a mouse model of MC903-induced atopic dermatitis. *Int Immunopharmacol*. 2019;74:105676. doi:10.1016/j.intimp.2019.105676
62. Takahashi N, Kake T, Hasegawa S, Imai M. Effects of post-administration of β-carotene on diet-induced atopic dermatitis in hairless mice. *J Oleo Sci*. 2019;68(8):793–802. doi:10.5650/jos.ess19092
63. Nasanbat B, Uchiyama A, Amalia SN, et al. Kaempferol therapy improved MC903 induced-atopic dermatitis in a mouse by suppressing TSLP, oxidative stress, and type 2 inflammation. *J Dermatol Sci*. 2023;111(3):93–100. doi:10.1016/j.jdermsci.2023.06.008
64. Generic diagramming platform (GDP): a comprehensive database of high-quality biomedical graphics | nucleic acids research | Oxford Academic. Available from: https://academic.oup.com/nar/article/53/D1/D1670/7848844. Accessed December 25, 2025.